

Lattice Dynamics of Diamond*

J. L. WARREN AND J. L. YARNELL

University of California, Los Alamos Scientific Laboratory, Los Alamos, New Mexico

AND

G. DOLLING AND R. A. COWLEY

Chalk River Nuclear Laboratories, Chalk River, Ontario, Canada

(Received 9 December 1966)

The first two authors have measured the dispersion curves for phonons whose wave vector lies along the symmetry lines Σ and Z in the Brillouin zone. The measurements were made by the method of inelastic neutron scattering. With the aid of these new results the latter two authors have determined the shell-model parameter δ which could not be determined from the previously measured dispersion curves along the lines Δ and A . A figure is given which summarizes all the measured dispersion curves of diamond and gives the most recently calculated shell-model fit to the data. Because of the large size of this parameter δ , it was necessary to recompute some of the thermodynamic and optical properties of diamond previously reported by the last two authors elsewhere. Thermodynamic quantities such as the Debye temperature were very little affected, but some of the critical-point frequencies used in the analysis of the two-phonon infrared absorption spectrum had to be altered. A corrected table of critical points is given.

INTRODUCTION

THE first two authors have previously reported measurements on the dispersion relation for phonons in diamond made by the method of inelastic neutron scattering.¹ These measurements were made for phonons whose propagation vector lies along the symmetry lines Δ , $\mathbf{q}=2\pi(\zeta,0,0)/a$, $0<\zeta<1$, and A , $\mathbf{q}=2\pi(\zeta,\zeta,\zeta)/a$, $0<\zeta<\frac{1}{2}$, in the Brillouin zone; $a=3.5672$ Å is the cubic lattice constant of diamond. The latter two authors subsequently wrote a paper on the thermodynamic and optical properties of germanium, silicon, diamond, and gallium arsenide.² In this paper they presented a least-squares fit of the above-mentioned data using a dipole-approximation model. They also predicted the dispersion relation for the symmetry lines Σ , $\mathbf{q}=2\pi(\zeta,\zeta,0)/a$, $0<\zeta<1$, and Z , $\mathbf{q}=2\pi(1,\zeta,0)/a$. These predictions could only be tentative because there was one parameter called δ in the model which could not be determined from the data along the lines Δ and A . In the predictions this parameter was set equal to zero. Under the assumption that this parameter was zero the latter two authors went on to calculate various thermodynamic and optical properties of diamond.

The purpose of this paper is twofold. We would like to report additional measurements made in Los Alamos for phonons propagating along the lines Σ and Z . With the aid of these new results the model parameter δ has been determined at Chalk River and some of the thermodynamic and optical properties of diamond have been recomputed. As previously these measurements were made by the method of neutron inelastic scatter-

ing. Since a description of the method of measurement and of the apparatus was given in Ref. 1, it will not be repeated here. A discussion of the theory and use of slow neutrons as a tool in the measurement of dispersion curves may be obtained from a book edited by Egelstaff.³

The next section will describe the diamond sample and compare it with the sample used in the previous experiment. The experimental results appear in the third section in the form of a figure and two tables. The fourth section discusses the method used to obtain the theoretical fit to the data and points out what effect this fit has on the conclusions of Ref. 2. In particular, a corrected table of two-phonon critical points is given.

THE SAMPLE

The measurements were made on the Oppenheimer diamond which was borrowed from the Smithsonian Institute in Washington, D. C. This diamond is a 253.7-carat, pale yellow, uncut, gem quality, single crystal, which is roughly octohedral in shape. Infrared and ultraviolet absorption measurements showed it to be a type-I diamond. The mosaic spread as measured by neutron diffraction was approximately 0.22° . This is a factor of five smaller than the mosaic spread of the sample used in the previous experiment. The previous sample was a 242.8-carat, light brown, uncut, industrial grade, type-II, nearly single crystal with a somewhat irregular shape.⁴ There were two small regions mis-oriented by 3° and 5° . Typeness in diamond is believed to be associated with the presence of substantial nitrogen.⁵ Type-I diamonds have more nitrogen than type-II. There is good evidence that the phonon dispersion

* Work supported in part by the U. S. Atomic Energy Commission.

¹ J. L. Warren, R. G. Wenzel, and J. L. Yarnell, in *Inelastic Scattering of Neutrons* (International Atomic Energy Agency, Vienna, 1965), Vol. I, p. 361.

² G. Dolling and R. A. Cowley, *Proc. Phys. Soc. (London)* **88**, 463 (1966).

³ *Thermal Neutron Scattering*, edited by P. A. Egelstaff (Academic Press Inc., New York, 1965), Chaps. 1, 3, and 5.

⁴ Contrary to what was stated on p. 235 of Ref. 3, this was not a synthetic diamond.

⁵ R. Berman, *Physical Properties of Diamond*, edited by R. Berman (Clarendon Press, Oxford, 1965), Chap. 11, p. 295-300.

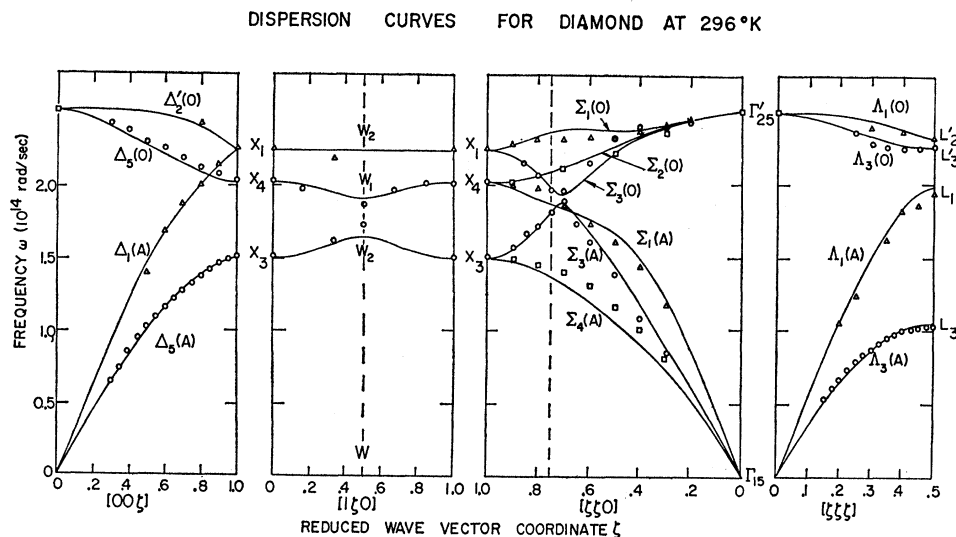


FIG. 1. The dispersion relation for the normal modes of vibration of diamond in the principal symmetry directions at 296°K. The full curves represent a shell-model fit to the data points. Branches and end points are labeled by the irreducible representations according to which the associated polarization vectors transform.

curves are a bulk property and very little affected by even large impurity concentrations.⁶ In order to check the sample independence of the dispersion curve previously measured, we repeated some points in the Δ direction and obtained agreement with the earlier numbers to within the estimated experimental error.

EXPERIMENTAL RESULTS

For ease of analysis, Fig. 1 gives all the measured dispersion curves for diamond, and also the most recent shell-model fit to the results.⁷ The experimental data for the Σ and Z directions are given in Tables I and II. The data for the Δ and Λ directions are to be found in Ref. 1. Estimates of the errors have not been placed on Fig. 1 but have been included in the tables for each individual point. These errors are somewhat larger than those obtained in the Δ and Λ directions. One reason for this is that the peaks in the scattered-neutron-intensity-versus-phonon-frequency curves did not always have symmetrical shapes. This made it difficult to assign a precise number for the frequency. Also many of the optical phonons gave rather broad peaks.

The branches of the dispersion curves in Fig. 1 are labeled by the names, in the notation of Koster,⁸ of the irreducible representations of the group of the wave vector. The polarization vectors of these normal modes transform, under the symmetry operations of the group of the wave vector, according to these representations. Since group theory was used not only to obtain these labels, but also to decide on the connectivity of the branches in the Σ direction, we will briefly outline its

application. For more detailed accounts of the use of group theory in solid-state physics we refer to the literature.⁹

For each wave vector of interest a six-dimensional representation of the group of the wave vector was obtained in a carrier space spanned by the displacements of the two atoms in the unit cell of diamond. The projection-operator¹⁰ method was used to reduce this representation into a direct sum of irreducible representations, and to obtain the form of the polarization vector associated with each irreducible representation. By examining the transformation properties of the polarization vectors, it was shown that the modes Δ_1 , Δ_2' , and Λ_1 are pure longitudinal, that Δ_5 and Λ_3 are doubly degenerate pure transverse, and that Σ_2 and Σ_4 are pure transverse polarized normal to a $(1\bar{1}0)$ plane. Also, Δ_1 and Σ_4 are acoustic, Δ_2' and Σ_2 are optic, and Δ_5 , Λ_1 , Λ_3 , Σ_1 , and Σ_3 each have both an optic and an acoustic branch. These modes were identified by selecting the conditions of the experiment so that only the desired mode would be detected. The remaining modes were identified by the use of compatibility relations¹¹ and the fact that branches belonging to the same representation cannot cross. Group theory would allow interchange of the labels L_1 and L_2' and of $\Sigma_1(O)$ and $\Sigma_3(O)$. The labeling for these two cases is based on an examination of the calculated eigenvectors of the shell model used to fit the data; the remaining identifications are independent of any particular model, being based only on group theory and experiment. It should

⁶ G. Dolling, in *Inelastic Scattering of Neutrons* (International Atomic Energy Agency, Vienna, 1965), Vol. I, p. 249.

⁷ The curves for the Δ and Λ directions have appeared previously in Ref. 2, but the curves for Σ and Z are new.

⁸ G. F. Koster, in *Solid State Physics*, edited by F. Seitz and G. Turnbull (Academic Press Inc., New York, 1957), Vol. 5, p. 173.

⁹ See, for example, M. Hamermesh, *Group Theory* (Addison-Wesley Publishing Company, Inc., London, 1962); M. Tinkham, *Group Theory and Quantum Mechanics* (McGraw-Hill Book Company, Inc., New York, 1964); M. Lax, *Symmetry Principles in Solid-State Physics* (to be published).

¹⁰ R. McWeeny, *Symmetry—An Introduction to Group Theory* (The MacMillan Company, New York, 1963), Chap. 5, p. 131.

¹¹ J. C. Slater, *Quantum Theory of Molecules and Solids* (McGraw-Hill Book Company, Inc., New York, 1965), Vol. 2, pp. 368–382.

TABLE I. Frequency ω (in units of 10^{14} rad/sec) versus reduced wave vector q/q_{\max} (dimensionless) for phonons propagating the Σ , $[110]$, direction in diamond.

q/q_{\max}	$\omega[\Sigma_4]$	$\omega[\Sigma_3(A)]$	$\omega[\Sigma_1(A)]$	$\omega[\Sigma_3(O)]$	$\omega[\Sigma_2]$	$\omega[\Sigma_1(O)]$
0.2				2.45 ± 0.03		2.46 ± 0.08
0.3	0.82 ± 0.03	0.85 ± 0.05	1.18 ± 0.08	2.41 ± 0.03	2.37 ± 0.02	2.42 ± 0.04
0.4	1.01 ± 0.02	1.09 ± 0.09	1.44 ± 0.04	2.40 ± 0.07		2.37 ± 0.03
0.5	1.17 ± 0.02	1.39 ± 0.05	1.61 ± 0.03	2.32 ± 0.02	2.22 ± 0.02	2.32 ± 0.06
0.6	1.31 ± 0.02	1.62 ± 0.04	1.74 ± 0.02	2.15 ± 0.02		2.34 ± 0.10
0.65		1.74 ± 0.04				
0.7	1.41 ± 0.03	1.87 ± 0.03	1.85 ± 0.02	1.97 ± 0.02	2.11 ± 0.04	2.32 ± 0.06
0.75		1.83 ± 0.03		1.97 ± 0.04		
0.8	1.46 ± 0.05	1.72 ± 0.01	1.98 ± 0.02	2.07 ± 0.03		2.32 ± 0.04
0.85		1.67 ± 0.07		2.15 ± 0.03		
0.9	1.50 ± 0.07	1.58 ± 0.09	2.00 ± 0.04		2.02 ± 0.04	2.28 ± 0.04
1.0	1.52 ± 0.06	1.52 ± 0.06	2.02 ± 0.05	2.23 ± 0.04		2.23 ± 0.04

be pointed out, however, that one can shortcut the projection-operator method for obtaining the polarization vectors by calculating the eigenvectors of the dynamical matrix from some model. One then uses the transformation properties of these eigenvectors to establish the labeling. This is in fact the way the labels were obtained in Ref. 2. The importance of these considerations can be demonstrated by reference to the work of Kucher and Nechiporuk.¹² Their dispersion curves are not consistent with the compatibility relation at X_1 , and hence the connectivity of their branches in the Σ direction must be in error.

THEORETICAL IMPLICATIONS

A shell model for diamond² was deduced before experimental results were available for the Σ direction. In this model a second-neighbor force constant δ could not be determined because it does not influence the frequencies of the normal modes in the Δ and Λ directions, and consequently was arbitrarily set to 0. The new measurements enable a value for this parameter to be deduced. The procedure used was to calculate the frequencies of the two Σ_3 modes of wave vector $(0.75, 0.75, 0)$ $2\pi/a$ for various values of δ while keeping the other parameters fixed. Comparison with the experimental results, Table I, then gives a value of δ of 4.75 (in units of e^2/v). This is considerably larger than the values of δ for germanium and silicon.² The model then gives reasonable agreement with the experimental results as shown in Fig. 1. Presumably it would

TABLE II. Frequency ω (in units of 10^{14} rad/sec) versus ζ (dimensionless) for phonons propagating along the symmetry line Z of the Brillouin zone of diamond. $\mathbf{q} = 2\pi(1, \zeta, 0)/a$. L stands for lower, M for middle, and U for upper.

ζ	$\omega[Z(L)]$	$\omega[Z(M)]$	$\omega[Z(U)]$
0.16		1.98 ± 0.10	
0.33	1.62 ± 0.02		2.2 ± 0.1
0.50	1.73 ± 0.02	1.87 ± 0.1	
0.67		1.97 ± 0.06	
0.84		2.01 ± 0.06	

¹² T. I. Kucher and V. V. Nechiporuk, Fiz. Tverd. Tela 8, 317 (1966) [English transl.: Soviet Phys.—Solid State 8, 261 (1966).]

be possible to obtain a better fit to all the results by allowing all the parameters to vary in an extension of the least-squares method described in Ref. 2. In particular, one might expect to achieve some improvement in the fit to the $\Sigma_4(A)$ branch in this way. Such a recalculation would probably result in only a slight improvement in the over-all fit, however, and we have not attempted this.

The change in the frequencies of the model for diamond necessitates the recalculation of the optical and thermodynamic properties of diamond. However, since the frequencies of only a few modes are changed significantly, the calculations of those properties, which depend on averages over the whole Brillouin zone, are

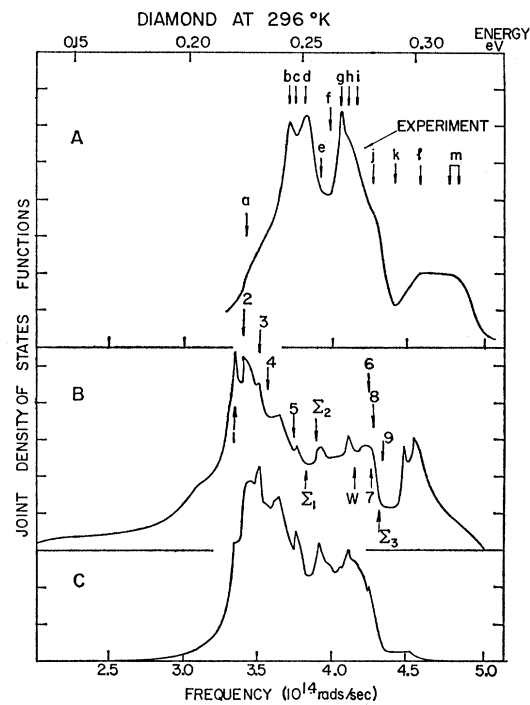


FIG. 2. Joint density-of-states functions for diamond at 296°K. Curve A is the experimental infrared absorption, curve B is a joint density of states, and curve C the infrared spectrum calculated with second-nearest-neighbor interactions. A detailed description of these different calculations is given in Ref. 2.

TABLE III. Critical-point analysis of infrared absorption in diamond. The kink positions (a to m) are those listed by Hardy and Smith.^a Frequencies are given in 10^{14} rad/sec. The code letters refer to Fig. 2, curves A and B.

Kink positions, curve-A code	Frequency	Assignments, curve-B code	Modes	Model calculation	Neutron data
a	3.42	2	LOTA (<i>L</i>)	3.40	3.38
b	3.71	4	ML (<i>W</i>)	3.55	3.60
c	3.75	5	LTA (<i>X</i>)	3.74	3.75
d	3.81	Σ_1	$\Sigma_2 O \Sigma_3 A$	3.81	3.83
e	3.92	Σ_2	UL (<i>W</i>)	3.88	(3.92) ^b
f	3.98	...	(Unknown)		
g	4.06	<i>W</i>	UM (<i>W</i>)	4.14	(4.07)
h	4.10	...	(Unknown)	4.11 ^c	
i	4.16	6	$\Sigma_1 O \Sigma_3 A$	4.24	4.19
j	4.27	7	LTO (<i>X</i>)	4.26	4.26
		or 8	TOLA (<i>L</i>)	4.27	4.23
k	4.42	9	LOLA (<i>L</i>)	4.34	4.29
		or Σ_3	$\Sigma_1 O \Sigma_3 O$	4.31	4.29
l	4.59	...	(Unknown)		
m	4.81 ^d	1		4.83	4.84
Not observed		...	TOTA (<i>L</i>)	3.34	3.32
Not observed		3	TOTA (<i>X</i>)	3.51	3.54

^a J. R. Hardy and S. D. Smith, *Phil. Mag.* **6**, 1163 (1961).

^b A bracketed figure in the final column indicates an estimated "experimental" value.

^c Combination presumably arising from non-symmetry-point modes. (The assignment and footnote for kinks g and h could clearly be interchanged without significantly worsening the agreement.)

^d Probably a 3-phonon combination $TA(X) + TA(L) + TO(L)$; some of the other features may also arise from 3-phonon contributions.

hardly altered by the use of the new model. The thermal expansion and specific heat are examples of these properties. One property which is altered however, is the location of the critical points. In particular, Fig. 2 shows a recalculation of the two-phonon infrared absorption spectrum for comparison with Fig. 8 of Ref. 2.

The frequencies of the critical points and one possible scheme of identification are given in Table III. Since the errors on the experimental measurement of the phonon frequencies are comparable to the differences between the frequencies of the critical points in the infrared spectra, this identification is at best only tentative; nevertheless, we believe it to be substantially correct.

The new model has also been used to calculate the frequency distribution and the results are very similar to those described earlier.² However, as with the infrared spectra, the critical-point frequencies are altered. Similar changes would occur in the Raman spectra.

ACKNOWLEDGMENTS

The first two authors gratefully acknowledge the cooperation of F. W. Taylor, Director of the Smithsonian Institution, and George Switzer, Chairman of the Department of Mineral Sciences of the same institution, in making the Oppenheimer diamond available for this investigation. They would also like to thank Norris Bradbury, Director of Los Alamos Scientific Laboratory, Peter M. Petersen of the Supply and Property Division of LASL, William F. Jenike, Chief of Procurement and Property Section of the Los Alamos Area Office of the AEC, and William Thomas of the Washington office of AEC for arranging the loan. The first author wishes to thank the Neutron-Physics Branch of the Chalk River Nuclear Laboratories for their hospitality during his visit. Finally we would like to acknowledge the help of R. G. Wenzel in the alignment of the crystal.